

# DALAResNet50 for Automatic Histopathology Breast Cancer Image Classification with DT Grad-CAM Explainability

SUXING LIU<sup>1,2†</sup>

<sup>1</sup>School of Computer Sciences, Universiti Sains Malaysia, Penang 11800, Malaysia

<sup>2</sup>School of Digital Arts, Jiangxi Arts & Ceramics Technology Institute, Jindezhen 33001, China

Corresponding author: Anusha Achuthan (anusha@usm.my)

arXiv:2308.13150v9 [eess.IV] 27 May 2024

## ABSTRACT

Automatic breast cancer classification in histopathology images is crucial for precise diagnosis and treatment planning. Recently, classification approaches based on the ResNet architecture have gained popularity for significantly improving accuracy by using skip connections to mitigate vanishing gradient problems, thereby integrating low-level and high-level feature information. Nevertheless, the conventional ResNet architecture faces challenges such as data imbalance and limited interpretability, necessitating cross-domain knowledge and collaboration among medical experts. This study effectively addresses these challenges by introducing a novel method for breast cancer classification, the Dual-Activated Lightweight Attention ResNet50 (DALAResNet50) model. It integrates a pre-trained ResNet50 model with a lightweight attention mechanism, embedding an attention module in the fourth layer of ResNet50 and incorporating two fully connected layers with LeakyReLU and ReLU activation functions to enhance feature learning capabilities. The DALAResNet50 method was tested on breast cancer histopathology images from the BreakHis Database across magnification factors of 40X, 100X, 200X, and 400X, achieving accuracies of 98.5%, 98.7%, 97.9%, and 94.3%, respectively. It was also compared with established deep learning models such as SEResNet50, DenseNet121, VGG16, VGG16Inception, ViT, Swin-Transformer, Dinov2\_Vitb14, and ResNet50. The reported results of DALAResNet50 have been shown to outperform the compared approaches regarding accuracy, F1 score, IBA, and GMean, demonstrating significant robustness and broad applicability when dealing with different magnifications and imbalanced breast cancer datasets. Additionally, to address the interpretability challenges, we introduce the Dynamic Threshold Grad-CAM (DT Grad-CAM) method. DT Grad-CAM enhances the traditional Grad-CAM approach by applying adaptive thresholding using Otsu's method, providing clearer and more focused visualizations of significant regions. This method improves the clarity and relevance of the highlighted areas, making it easier for medical experts to interpret the model's predictions and understand the critical features contributing to the classification. The integration of DT Grad-CAM with DALAResNet50 not only ensures high classification performance but also offers enhanced interpretability, crucial for reliable and transparent breast cancer diagnosis.

**INDEX TERMS** Lightweight attention mechanism, Convolutional Neural Networks, breast cancer classification.

## I. INTRODUCTION

Breast cancer has become a leading cause of mortality, particularly among women, with its incidence rising continuously, raising global health concerns [1], [2]. Early, accurate diagnosis and treatment are pivotal in decreasing the mortality rate associated with breast cancer. Yet, medical practices face challenges such as insufficient healthcare resources and

human error in interpretation, which impede the timely and precise detection and diagnosis of breast cancer. Against this backdrop, intelligent diagnostic assistance technologies have emerged as innovative solutions in the battle against breast cancer. Recent advances in deep learning have revolutionized breast cancer diagnosis, surpassing the limitations of traditional classification and recognition algorithms by integrating

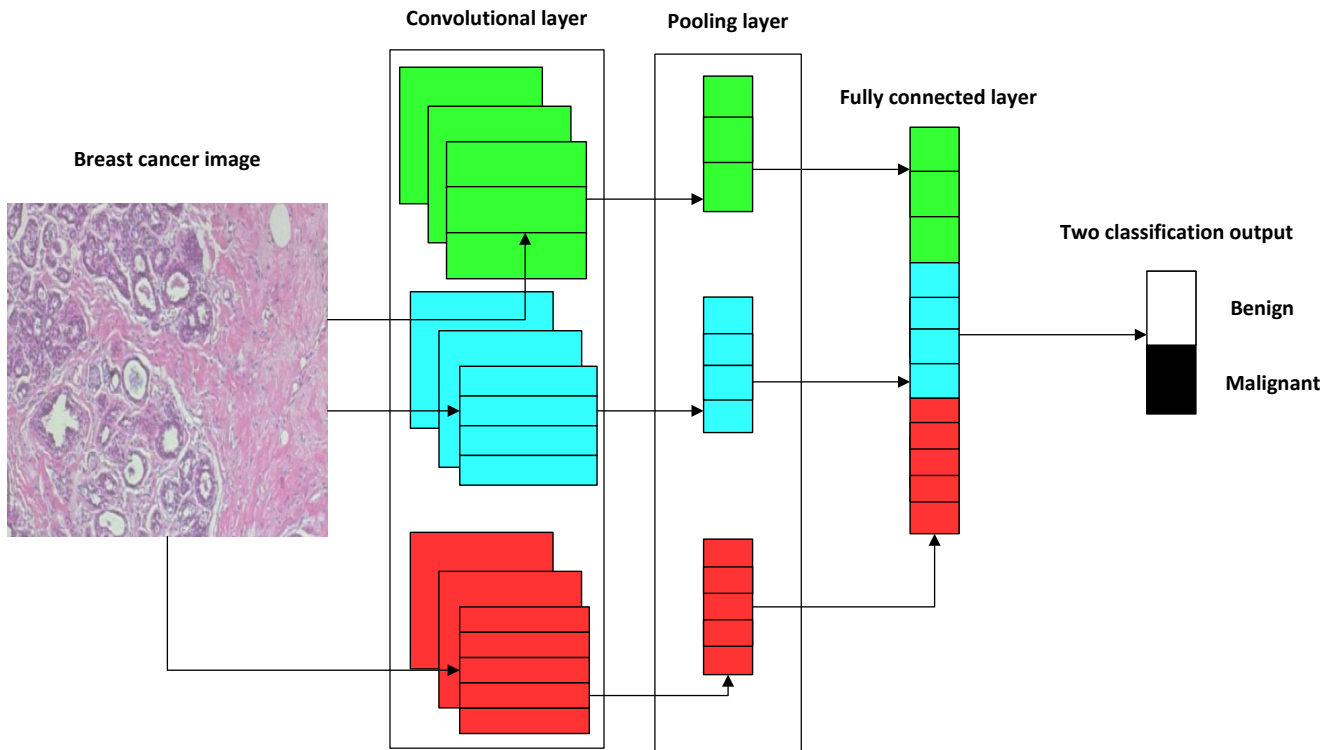


FIGURE 1. Overview of Convolutional Neural Network

feature extraction, selection, and classification into a unified step. Deep learning automates feature extraction and classification through neural networks, reducing redundancy and enhancing efficiency, thus significantly improving diagnostic accuracy and workflow [3]–[7]. A pivotal innovation in this domain is developing and applying Convolutional Neural Networks (CNNs), specialized deep learning models adept at processing data, such as medical images, with a grid-like topology. In 1998, LeCun et al. [8] introduced Convolutional Neural Networks (CNNs), which progressively extract abstract features from images through multiple levels of convolutional and pooling operations. This process enables CNNs to achieve classification based on these extracted features. CNNs comprise convolutional, pooling, and fully connected layers, collaboratively facilitating the robust classification of medical images. The convolutional layer identifies local image features; the pooling layer reduces data dimensions while retaining critical information; and the fully connected layer maps these features to output classes, as illustrated in Fig. 1. Despite deep learning's significant achievements in medical image classification, conventional CNN architectures often struggle with imbalanced medical image data. This paper proposed a Dual-Activated Lightweight Attention ResNet50 (DALAResNet50) model designed to overcome the challenge of imbalanced data in CNN architectures. This innovative approach efficiently manages uneven category distributions

and enhances the detection of malignant breast cancer in medical images. The primary contributions of this work are summarized as follows:

(a) This study introduces a novel lightweight attention mechanism network that adaptively adjusts channel feature extraction to enhance feature representation. This approach optimizes the network's ability to discern relevant features for breast cancer classification.

(b) Integrating the attention mechanism with ResNet50 [9] creates a feature-rich model, achieving more efficient feature extraction by combining the strengths of both techniques. Specifically, within the attention mechanism's fully connected network component, LeakyReLU [10] and ReLU [11] activation functions are employed. LeakyReLU is chosen for its capability to alleviate the issue of vanishing gradients; ReLU is used to improve the representation of image features, facilitating the capture of multi-scale spatial patterns more effectively.

(c) The paper tests images at various magnifications, demonstrating the network's scale invariance and superior performance over other contemporary methods.

(d) The model undergoes comprehensive evaluation, focusing on analyzing loss. The findings indicate stable performance during the later stages of training, effectively minimizing overfitting and demonstrating strong generalization capabilities for new data.

Organization of the paper:

Section II reviews the latest advancements in applying deep learning for breast cancer diagnosis.

Section III proposed the DALAResNet50 model approach for classifying breast cancer histopathology images.

Section IV outlines the dataset and implementation specifics of the experimental setup and compares the classification outcomes with those of other leading networks.

Section V conducts an in-depth performance evaluation of the model through loss and accuracy analysis.

Section VI provides a summary and conclusions.

## II. RELATED WORKS

Cancer tissue histopathology image classification predominantly utilizes traditional manual feature extraction and deep learning-based methods. Traditional approaches depend on manually extracting features from images and employing classifiers such as SVM (Support Vector Machine) or Random Forest for recognition. However, these methods encounter limitations, such as the need for intensive feature extraction, a requirement for substantial domain knowledge, and challenges in acquiring high-quality features [12]. In contrast, deep learning-based methods, mainly through models like Convolutional Neural Networks (CNNs), offer a more efficient feature extraction process [13]. Specifically, deep learning approaches to cancer tissue histopathology image classification include CNN-based, transfer learning-based, and attention mechanism-based breast cancer classification. Each of these methods leverages the inherent strengths of deep learning to improve classification performance, which will be explored in detail in the subsequent section.

### A. CNN

CNN, one of the most widespread deep learning techniques, excels in image processing tasks [14]. They utilize convolutional, pooling, and fully connected layers to learn and classify image features effectively [15]. In breast cancer histopathology image classification, CNN models like AlexNet, Inception, VGGNet, DenseNet, and ResNet have demonstrated substantial capabilities when trained on large datasets.

AlexNet, introduced in 2012 by Alex et al. [16], represented a significant milestone in ImageNet competition history, showcasing the potent capabilities of CNNs. Modified versions of AlexNet, such as the one by Omonigho et al. [17] on the MIAS mammography database, achieved notable accuracy, indicating superior performance over traditional methods. However, challenges remain in parameter optimization and application to imbalanced datasets.

The Inception model, developed by Google, addresses computational and parameter efficiency in neural networks, making it ideal for image classification tasks. Nazir et al.'s hybrid CNN-Inception-V4 model [18] demonstrated high accuracy and sensitivity, though it faced limitations in specificity and computational efficiency considerations.

VGGNet, crafted by Oxford University researchers, excels in image classification but is less suited for resource-constrained

environments due to its intensive computational and memory demands. Nedjar et al. [19] presented a visualization method for VGG19's decision-making process in breast biopsy image classification, enhancing medical professionals' trust and CNN efficiency.

DenseNet [20], known for its efficient information and gradient flow through dense connectivity, offers advantages in overcoming challenges like gradient vanishing. Jiménez Gaona et al. [21] leveraged DenseNet for breast cancer detection, showing its superiority in reducing parameters and improving performance compared to other CNN architectures.

ResNet, introduced by He et al. in 2015 [9], addresses deep neural networks' vanishing gradient problem, allowing for the construction of deeper networks. An enhanced capsule network using Res2Net blocks, proposed by Khikani et al. [22], demonstrated improved performance in breast cancer classification, although ResNet-50 faces challenges with imbalanced datasets. This paper presents modifications to the ResNet50 model to tackle these issues, given its accuracy advantage over other methods.

### B. TRANSFER LEARNING

Transfer learning applies pre-trained models from one image domain to another, bridging the gap between different image domains. In the context of breast cancer image classification, this pre-trained model approach involves fine-tuning CNN models, which were initially trained on a comprehensive large-scale image dataset, and then fine-tuning it to adapt to the dataset used explicitly for breast cancer detection. This step optimizes the model better to meet the specific needs of breast cancer classification. By using the inherent ability of the pre-trained model in generalization and feature extraction, this strategy significantly improves the efficiency of training and the accuracy of classification performance [23]–[29].

Ismail et al. [30] used transfer learning to expedite model training. Using models like VGG16 and ResNet50, they classified breast cancer images. Their experiments confirmed that transfer learning quickens model convergence and outperforms training from scratch.

Muhammad et al. [31] also utilized pre-trained deep learning models for breast cancer detection, such as ResNet50, ResNet101, VGG16, and VGG19. After training and testing these models on a dataset of 2453 breast histopathology images, they found that ResNet50 had a superior performance with an accuracy rate of 90.2%, an Area Under the Curve (AUC) of 90.0%, and a recall rate of 94.7%.

In conclusion, this study has focused on further optimization and enhancement due to the exceptional robustness of ResNet50 in transfer learning. Nevertheless, the investigation encounters specific challenges when dealing with imbalanced breast cancer datasets. Firstly, the imbalance in the dataset tends to bias the model towards categories with a larger number of instances, potentially leading to a significant reduction in the detection rate of key but less frequent categories, especially in early-stage breast cancer cases, thereby increasing the risk of missed diagnoses. Secondly, given the limited sam-

ple size of minority categories, there is a risk of overfitting in these samples, affecting the model's generalization ability for novel and previously unseen minority class samples. Therefore, this study aims to overcome these challenges by meticulously optimizing the application of ResNet50 in transfer learning, thereby enhancing the model's overall performance in dealing with imbalanced breast cancer data.

### C. ATTENTION MECHANISM

In medical imaging, the attention mechanism [32] in deep learning has emerged as a revolutionary technique. It allows models to allocate varying levels of importance to different regions within medical images, such as MRI scans, X-rays, CT scans, and histopathology images [33]. This selective focus enables the models to prioritize and scrutinize the most relevant areas for diagnosing diseases, detecting anomalies, or monitoring the progression of medical conditions. By zeroing in on essential features within these images, the attention mechanism significantly boosts the accuracy and efficiency of automated medical image analysis, contributing to early detection and enhanced patient outcomes. Within breast cancer image classification, incorporating the attention mechanism encourages the model to discern critical and distinctive features in breast cancer images that are pivotal for accurately differentiating between malignant and benign tissues. This strategy can elevate the model's performance, diminish reliance on global image feature extraction, and enhance the precision in pinpointing vital breast cancer regions [34].

Researchers have proposed various breast cancer segmentation and classification systems incorporating attention mechanisms. For example, Vardhan et al. [35] developed a breast cancer segmentation system utilizing Convolutional Neural Networks (CNNs) with interpretable artificial intelligence and the attention mechanism to enhance breast cancer detection and classification accuracy and speed. Xu et al. [36] designed a system for breast cancer segmentation employing a modified DenseNet architecture with an attention mechanism to refine the CNN's performance on the BreakHis dataset for high-precision breast cancer classification. This method was evaluated on the BreakHis dataset using accuracy metrics for both binary and multi-classification. Wang et al. [37] proposed a breast cancer classification model that combines deep transfer learning and visual attention mechanisms to increase the accuracy and efficiency of real-world clinical diagnoses. Based on deep transfer learning with attention mechanisms, this approach utilizes transfer learning to tackle the overfitting problem and integrates an attention module to concentrate on characterizing breast lesions. Wang et al.'s work achieves high-precision results that surpass other state-of-the-art breast image classification algorithms.

This section summarizes recent scholarly research and exploration of breast cancer classification, emphasizing the use of the attention mechanism. The insights indicate that applying the attention mechanism in breast cancer images and classification methods can simultaneously enhance the accuracy of crucial region identification and increase the model's inter-

pretability. However, this also correspondingly increases the following difficulties:

#### 1) Limitations in global feature extraction

Although the attention mechanism is designed to improve model performance by focusing on critical sections of the image, thereby playing a positive role in enhancing the model's ability to process global information of the image, it may still encounter challenges in some implementations or specific application scenarios, failing to grasp the entire image's global contextual details fully.

#### 2) Insufficiency in feature priority precision

Lacking a sophisticated method to discern the significance of diverse features, attention mechanisms might uniformly weigh all channel information. This approach risks overlooking vital features essential for precise classification, compromising the model's effectiveness in identifying and leveraging distinctive patterns in the data.

#### 3) Inefficiency of Activation Functions

The reliance on ReLU within attention mechanisms can lead to the "dying ReLU" issue, wherein neurons fail to activate over specific data ranges, stalling the learning progression. Such constraints significantly diminish the model's adaptability during the training phase, adversely affecting the dynamics and overall efficacy of the attention-enhanced learning process.

#### 4) Lack of feature adaptability

Attention mechanisms may exhibit rigidity in adjusting and enhancing features non-linearly according to the unique characteristics of each input. This inflexibility can constrain the model's ability to adapt and optimally leverage the diverse information within the data, thereby reducing the overall efficiency in feature utilization.

This study designed an innovative lightweight attention module to overcome the identified difficulties. This design incorporates adaptive average pooling, a two-layer fully connected network for channel recalibration, dual activation functions of LeakyReLU [10] and ReLU [11], and element-wise multiplication. Adaptive average pooling tackles the limitations in global feature extraction, whereas the two-layer fully connected network for channel recalibration optimizes feature priority precision. The combination of LeakyReLU and ReLU effectively addresses the inefficiencies of a single activation function, enhancing activation function efficiency, and element-wise multiplication improves feature adaptability. These pioneering approaches synergistically aim to significantly elevate model performance while mitigating computational resource requirements, providing a more efficient and adaptable solution for integrating attention mechanisms into breast cancer image classification models. Moreover, this paper presents a comparative analysis between the proposed DALAResNet50 model and the standard ResNet model, as illustrated in Table 2.

#### D. GRAD-CAM-BASED VISUALIZATION TECHNIQUES IN HISTOPATHOLOGY IMAGE ANALYSIS

Grad-CAM (Gradient-weighted Class Activation Mapping) is a widely used technique for visualizing the regions of an image that are most relevant to a neural network's predictions. This technique has been extensively explored in the field of histopathology image analysis to improve model interpretability and provide insights into the decision-making process of deep learning models [59].

In histopathology, accurate interpretation of tissue images is crucial for diagnosing diseases such as cancer. Traditional Grad-CAM methods generate heatmaps by computing the gradients of the target class with respect to the feature maps of the last convolutional layer, highlighting the regions of the image that contribute most to the classification decision. This allows pathologists to understand which areas of the tissue image the model focuses on, aiding in verifying the model's predictions.

However, conventional Grad-CAM has limitations, particularly in dealing with noisy activations and less distinct regions, which can hinder the clarity and precision of the visualizations. Various enhancements have been proposed to address these challenges. For instance, Guided Grad-CAM combines Grad-CAM with guided backpropagation to produce high-resolution class-discriminative visualizations, offering finer details of the important regions [60]. Additionally, Score-CAM removes the dependency on gradients by using the target class score, improving the heatmaps' stability and robustness [61]. “

To further enhance the interpretability and effectiveness of visual explanations in histopathology image analysis, we chose to implement the Dynamic Threshold Grad-CAM (DT Grad-CAM) method. DT Grad-CAM addresses the limitations of conventional Grad-CAM by applying adaptive thresholding using Otsu's method, which dynamically determines the optimal threshold for highlighting significant regions. This approach reduces noise and enhances the clarity of the visualizations, making it easier to identify and interpret the critical features that contribute to the model's predictions. By focusing on the most relevant areas and minimizing the influence of less important regions, DT Grad-CAM provides more precise and interpretable heatmaps, which are particularly beneficial in clinical settings where accurate and transparent decision-making is essential.

### III. METHODS

#### A. TRANSFER RESNET50

The ResNet50 [9] model has a relatively complex structure, including a 50-layer deep network structure. The specific structure is shown in Table 1. The primary module is made up of numerous residual blocks. Each block is equipped with multiple convolutional layers and distinctive identity maps. Uniquely, the ResNet50 model introduces the concept of residual learning. This innovation solves the problem of vanishing gradients in deep networks, thereby opening up the possibility of building deeper neural networks. This design breakthrough

TABLE 1. The ResNet50 Model

Module Name	Output Size	50 Layers
Conv1	$112 \times 112$	$7 \times 7, 64$ stride=2
Conv2_x	$56 \times 56$	$\left\{ \begin{array}{l} 1 \times 1, 64 \\ 3 \times 3, 64 \\ 1 \times 1, 256 \end{array} \right\} \times 3$
Conv3_x	$28 \times 28$	$\left\{ \begin{array}{l} 1 \times 1, 128 \\ 3 \times 3, 128 \\ 1 \times 1, 512 \end{array} \right\} \times 4$
Conv4_x	$14 \times 14$	$\left\{ \begin{array}{l} 1 \times 1, 256 \\ 3 \times 3, 256 \\ 1 \times 1, 1024 \end{array} \right\} \times 6$
Conv5_x	$7 \times 7$	$\left\{ \begin{array}{l} 1 \times 1, 512 \\ 3 \times 3, 512 \\ 1 \times 1, 2048 \end{array} \right\} \times 3$
Pooling	$1 \times 1$	Average Pool, 1000-d FC.
Note: The term "1000-d FC" in the pooling layer refers to a fully connected layer consisting of 1000 neurons.		

allowed for achieving promising performance. Therefore, the transfer learning strategy based on the pre-trained ResNet50 model is adopted in this paper, considering the efficient utilization of data and computing resources for model building. The benefit of transfer learning is the high-level feature representations learned by ResNet50 on large-scale datasets in medical image classification tasks. This allows for swiftly attaining superior classification outcomes, even with constrained data and computing capacities. As shown in Fig. 2, the proposed approach includes a histopathology breast cancer database and components for preprocessing and data augmentation, transfer learning based on ResNet50, and classification based on an improvised dual-activated fully connected layer. The proposed approach involves the following stages for breast cancer classification using histopathology images:

#### B. DUAL-ACTIVATED LIGHTWEIGHT ATTENTION RESNET50

A new approach for automatic breast cancer classification is proposed in this research using a new version of the ResNet50 technique called Dual-activated lightweight attention ResNet50 (DALAResNet50). The DALAResNet50 model is methodically structured into three core stages: data preprocessing and augmentation, transfer learning based on ResNet50 architecture, and DALAResNet50 model optimization, as detailed below:

##### 1) Data preprocessing and augmentation

Initially, all breast cancer histopathology images are resized to  $224 \times 224$  pixels, aligning with the input specifications for convolutional neural networks. A normalization process follows, adjusting pixel values to a range between  $[-1, 1]$  to expedite model training and augment the model's generalization capability with novel data. Data augmentation strategies like random rotation and horizontal flipping bolster the model's robustness. These strategies mimic potential real-world image alterations, improving the model's resilience to subtle image variations.

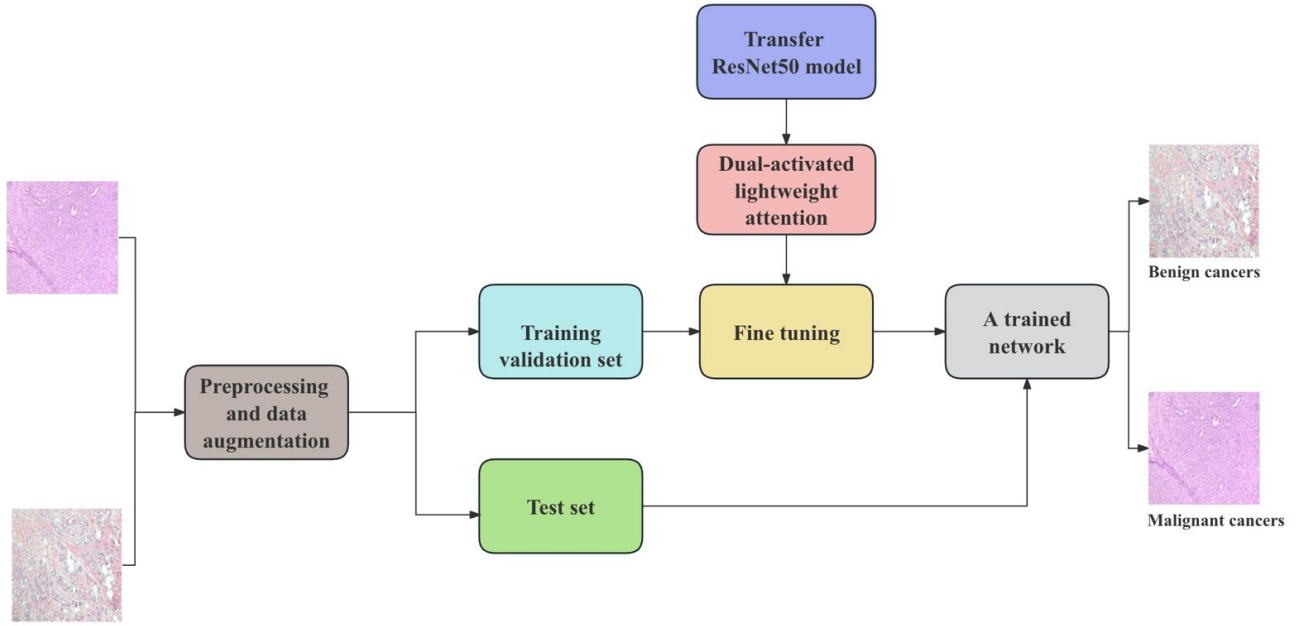


Fig. 2. The framework of DALAResNet50 model

## 2) Transfer learning based on ResNet50

At this stage, capitalizes on a pre-trained ResNet50 framework, incorporating a custom-designed attention module within its fourth residual block. This module aims to pinpoint small-scale cell nuclei characteristic of breast cancer and glean pertinent semantic information. This strategic enhancement significantly boosts the model's ability to learn and discern features.

## 3) DALAResNet50 model optimization

During the optimization phase of the DALAResNet50 model, a sequential focus is placed on pooling layers, activation layers, and nonlinear feature adjustments to enhance the model's performance and adaptability. The related steps are as follows:

- 1) Initially, to address the issue of spatial variations in input feature maps, traditional pooling layers are replaced with adaptive average pooling. This adjustment optimizes the network's parameter structure, enabling the model to process global contextual information more effectively and accurately. The introduction of adaptive average pooling not only simplifies the network's complexity but also enhances the model's ability to capture important information from different parts of the image, laying a solid foundation for subsequent feature processing. Specifically, the adaptive average pooling operation is defined as follows:

$$y_i = \frac{1}{H_i \times W_i} \sum_{h=1}^{H_i} \sum_{w=1}^{W_i} x_{i,h,w} \quad (1)$$

where  $y_i$  is the output of the adaptive average pooling layer for the  $i$ -th feature map,  $H_i$  and  $W_i$  are the height and width of the  $i$ -th feature map, respectively, and  $x_{i,h,w}$  represents the value at position  $(h, w)$  in the  $i$ -th feature map. This approach establishes a solid foundation for subsequent feature processing, allowing the model to effectively capture and utilize global contextual information from the input images.

- 2) Next, the model employs a dual activation function strategy in the activation layer, starting with the LeakyReLU activation function [10] in the initial phase. This function is chosen for its unique capability to maintain a slight yet nonzero gradient when the unit is inactive, effectively combating the problem of vanishing gradients and significantly boosting the training efficiency of deep neural networks. The LeakyReLU activation function is defined as follows:

$$f(x) = \begin{cases} x & \text{if } x > 0 \\ \alpha x & \text{otherwise} \end{cases} \quad (2)$$

where  $f(x)$  represents the LeakyReLU function and  $\alpha$  is a small constant (typically 0.01) that allows a small gradient when the input  $x$  is negative. Following this, the ReLU activation function [11] is applied in the subsequent fully connected layer to optimize model performance further and enhance the representation of image features. The ReLU activation function is defined as:

$$f(x) = \max(0, x) \quad (3)$$

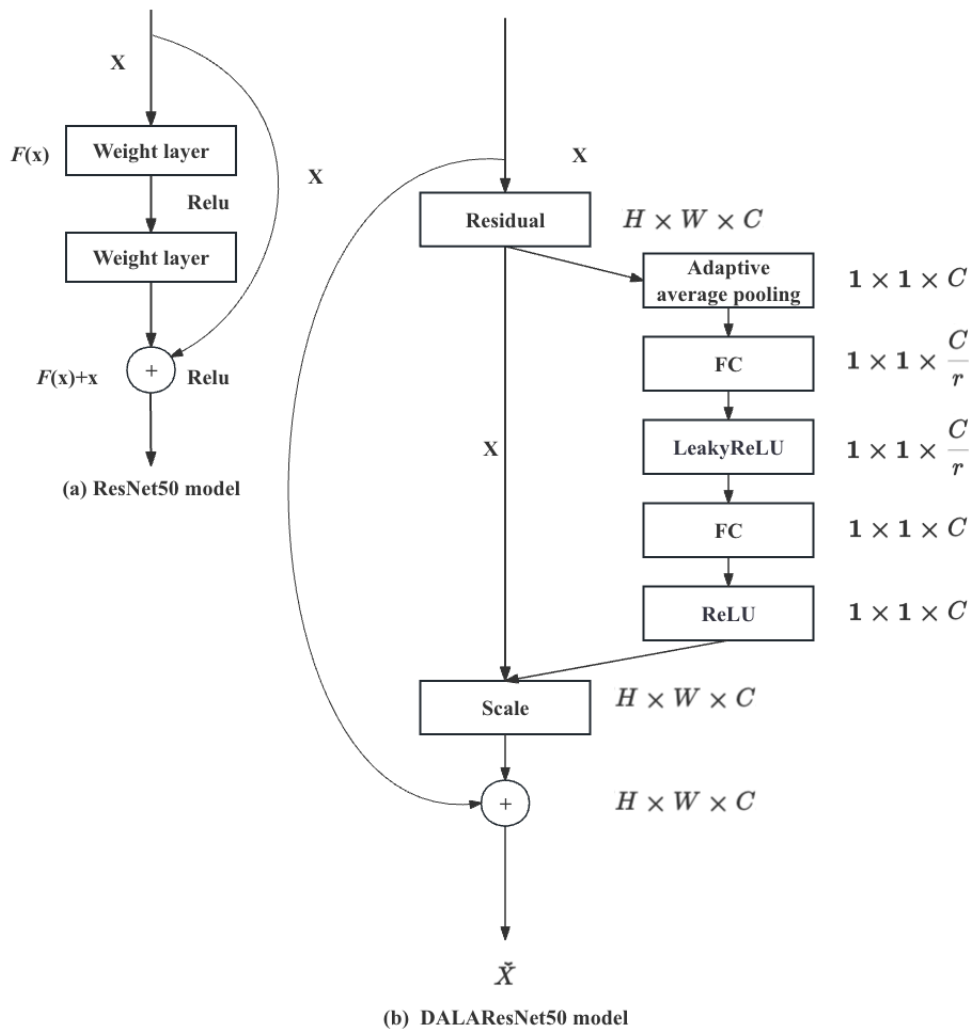


Fig. 3. Comparison of conventional ResNet50 and DALAResNet50 model: (a) ResNet50 model (b) DALAResNet50 model

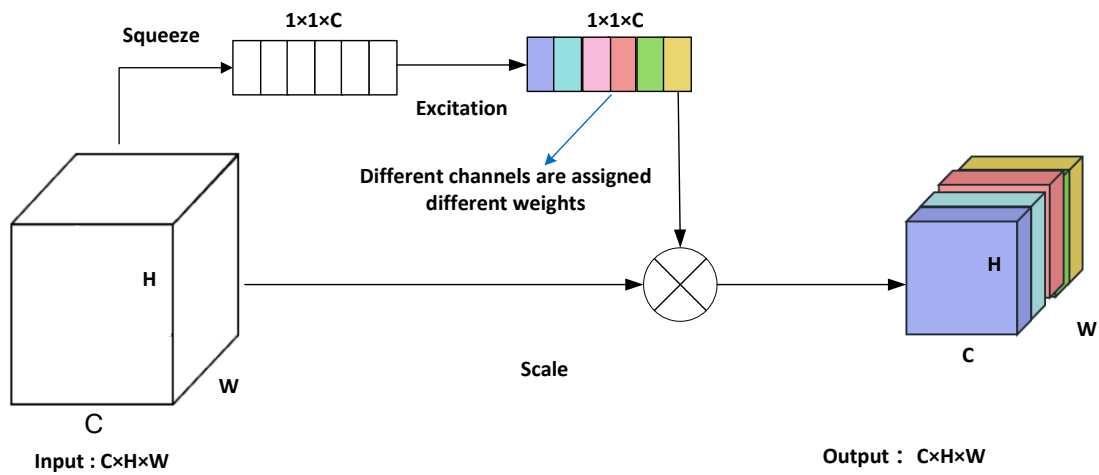


Fig. 4. Visualization of DALAResNet50 model

**TABLE 2. Comparison between DALAResNet50 model and standard ResNet model**

Feature	DALAResNet50 model	Standard ResNet model
Adaptive Average Pooling	Adaptive average pooling addresses "limitations in global feature extraction" by enhancing the model's capacity to process global contextual information, significantly improving performance in tasks requiring comprehensive image understanding.	Not available
Channel Recalibration	A two-layer fully connected network for channel recalibration optimize "feature priority precision," enhancing the model's ability to identify and focus on the most relevant features for accurate classification.	Not available
Activation Functions	The dual activation functions of LeakyReLU and ReLU address the "inefficiency of activation functions." By incorporating LeakyReLU, the network avoids the dying ReLU problem, as it allows a small, nonzero gradient when the unit is not active, ensuring continuous learning dynamics and preventing neurons from becoming inactive across all network layers. This combination maintains the model's learning capability, potentially enhancing the training process.	ReLU only
Element-wise multiplication	Element-wise multiplication, as denoted by 'Scale' in Fig. 3, enhance "Feature Adaptability" by allowing dynamic, nonlinear adjustment of features according to a specific input, improving the network's flexibility and utilization of information.	Not available

where  $f(x)$  is the ReLU function, which outputs  $x$  if  $x$  is positive and 0 otherwise. The careful combination of LeakyReLU and ReLU activation functions dramatically improves the model's ability to process and learn complex image characteristics, providing strong support for accurately classifying breast cancer images. By employing LeakyReLU in the initial phase, the model effectively addresses the vanishing gradient problem, while the subsequent use of ReLU enhances the network's nonlinearity and expressive power, thereby improving its overall performance and robustness.

3) Finally, the introduction of element-wise multiplication

operations further enhances the model's feature adaptability, allowing for dynamic, nonlinear adjustments of features based on specific inputs. This step significantly increases the network's flexibility and information utilization, enabling the model to adapt its processing flow according to the particular circumstances of the input features. This approach notably improves the model's feature processing capability, leading to higher accuracy and efficiency in classifying breast cancer images. The element-wise multiplication operation is defined as follows:

$$z_i = x_i \cdot y_i \quad (4)$$

where  $z_i$  is the result of the element-wise multiplication of the  $i$ -th feature map, and  $x_i$  and  $y_i$  are the corresponding elements of the feature maps being multiplied. This operation allows the model to adjust the features dynamically, enhancing its ability to capture complex patterns and interactions within the data.

Fig. 3 illustrates the flowcharts of the standard ResNet50 approach and the DALAResNet50 approach, respectively. These flowcharts highlight the newly added features in the DALAResNet50. Table 2 details a comprehensive comparative analysis of these differences. Fig. 4 depicts the visualization of the DALAResNet50 approach.

## IV. EXPERIMENT

### A. BREAKHIS DATASET

The BreakHis dataset, utilized in this study focusing on breast cancer histopathology images, was generously provided by scholar Spanha [38]. This dataset comprises histopathology samples of breast cancer tumors obtained from 82 patients. The samples were sectioned under a microscope and then imaged at different magnifications ( $40\times$ ,  $100\times$ ,  $200\times$ ,  $400\times$ ) to capture intricate details. Experienced medical professionals meticulously interpreted and identified the images. The dataset consists of a total of 7,909 breast cancer pathological images, comprising 2,429 benign tumor images and 5,429 malignant tumor images. Each image has dimensions of  $700 \times 460$  pixels and is stored in PNG format with three color channels. The detailed dataset statistics in Table 3 cover sample size, class distribution, etc. This multi-angle data resource provides a solid foundation for effective image classification and analysis research. In addition, to more intuitively display the breast cancer tissue details under different magnifications, Fig. 5 presents these pathological images as a practical example.

Since the BreakHis dataset is a publicly available dataset, this study does not require ethical approval. Additionally, publicly available datasets are typically subject to stringent quality control measures; therefore, this study does not separately consider image quality issues.



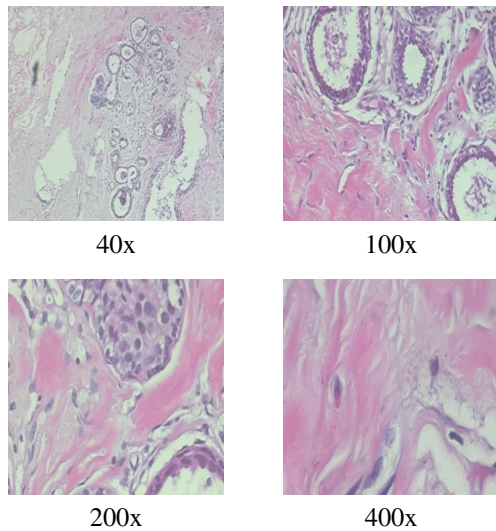


**Fig. 5.** Images of breast cancer pathology at four magnifications

**TABLE 3.** BreakHis dataset: benign and malignant image distribution across magnification factors

Class	Magnification Factor			
	40X	100X	200X	400X
Benign	625	644	623	588
Malignant	1370	1437	1390	1232
Total No of Images	1995	2081	2013	1820

## B. EXPERIMENTAL ENVIRONMENT

The experiments were carried out on an NVIDIA RTX A4000 GPU, utilizing the PyTorch 2.0.1 framework paired with Python 3.10.

## C. EXPERIMENT IMPLEMENTATION

This research utilizes a ratio of 6:1:3 to divide the processed dataset into training, verification, and test sets, as presented in Table 4. The training set is used for model training, during which parameter learning occurs. The verification set is employed to assess the model's generalization ability. Continuous verification and parameter fine-tuning ensure superior model performance, with the optimal model pre-trained during verification. The test set measures the model's recognition rate and generalization performance. Before model training, the training data is shuffled to enhance the model's robustness and generalization capabilities.

In deep learning, the configuration of various parameters is paramount. Notably, the learning rate plays a crucial role; an excessively high learning rate may result in the loss value exploding, while a meager learning rate may lead to overfitting and reduce the model's convergence speed. In previous studies, the initial learning rate is usually set in the range of 0.1 to 0.0001. Considering the relatively small size of the BreakHis medical imaging dataset (containing 7909 images) and the uneven distribution of the data, a lower learning rate of 0.0001 was chosen for this study so that the model could adjust the weights more accurately. This is important for dealing with small and imbalanced datasets to ensure that all categories

**TABLE 4.** Dataset split for experimental task

Split	Percentage	Purpose
Training	60%	Model Training
Validation	10%	Hyperparameter Tuning
Testing	30%	Model Evaluation

**TABLE 5.** Experimental configuration

Parameter	Value
Batch Size	32
Epochs	50
Learning Rate	0.0001
Dropout	0.25

are given proper attention. In addition, setting the training batch size and the number of iterations is significant. In addition, setting the training batch size and the number of iterations is substantial. Previous studies usually set the batch size between 32 and 128. Considering the GPU's 16GB video memory limit, the lowest batch size of 32 was chosen for this study. As for the number of iterations, it is also usually set between 50 and 128. Given the size of the BreakHis dataset, this study limited the number of iterations to 50, aiming to balance training effectiveness and computational efficiency. Finally, this study also specifically considered the dropout rate setting. Previous studies generally set the dropout rate between 0.25 and 0.5. In processing the imbalanced BreakHis dataset, a lower dropout rate helps ensure that the categories with smaller numbers are sufficiently learned, thus improving the model's recognition accuracy and generalization ability. Therefore, this study chose a lower dropout rate of 0.25.

The method proposed in this study and the benchmark model illustrated in Table 6 apply the above settings to ensure the experiments' fairness and the comparability of the results. These carefully selected parameters provide a solid foundation for the experimental design and ensure the reliability and efficiency of the model throughout the study; the parameter settings are shown in Table 5.

## D. BASELINE SELECTION

Table 6 presents a comparative analysis of various deep learning methods, encompassing widely adopted approaches and the novel strategy introduced in this paper. The following section briefly outlines several of the models included in the comparison:

**SEResNet50** [39]: Hu et al. proposed this model in 2018. The key feature of this model is integrating the "squeeze and excitation" attention mechanism, which aims to improve the network's capabilities.

**DenseNet-121** [40]: Huang et al. proposed this model in 2017 by introducing dense connections (dense blocks) to transfer and reuse information between network layers, thus improving the efficiency of feature transmission and reproduction. This study employs transfer learning with DenseNet-121, which is utilized for classifying breast cancer. The advantage of using a pre-trained DenseNet is that it can adapt to

**TABLE 6. Classification results of 9 network models**

Network Models	40X				100X			
	Accuracy	F1	IBA	GMean	Accuracy	F1	IBA	GMean
SEResNet50 [39]	0.883	0.779/0.883	0.860	0.860	0.850	0.720/0.849	0.813	0.812
DensNet121 [40]	0.801	0.639/0.800	0.763	0.762	0.811	0.654/0.809	0.755	0.753
VGG16 [41]	0.902	0.813/0.902	0.877	0.877	0.850	0.724/0.851	0.830	0.829
VGG16Inception [42]	0.977	0.955/0.977	0.965	0.965	0.971	0.943/0.971	0.964	0.964
ViT [43]	0.835	0.693/0.833	0.769	0.767	0.834	0.694/0.833	0.788	0.787
Swin-Transformer [44]	0.843	0.711/0.844	0.819	0.818	0.877	0.767/0.876	0.836	0.835
Dinov2_Vitb14 [45]	0.873	0.762/0.873	0.843	0.843	0.869	0.753/0.868	0.835	0.834
RseNet50 [9]	0.927	0.860/0.927	0.914	0.914	0.944	0.891/0.944	0.922	0.922
<b>DALAResNet50</b>	<b>0.985</b>	<b>0.970/0.985</b>	<b>0.980</b>	<b>0.980</b>	<b>0.987</b>	<b>0.974/0.987</b>	<b>0.985</b>	<b>0.985</b>

Network Models	200X				400X			
	Accuracy	F1	IBA	GMean	Accuracy	F1	IBA	GMean
SEResNet50 [39]	0.906	0.820/0.906	0.876	0.875	0.876	0.770/0.878	0.864	0.863
DensNet121 [40]	0.812	0.659/0.812	0.775	0.774	0.779	0.603/0.777	0.737	0.736
VGG16 [41]	0.851	0.722/0.850	0.812	0.811	0.848	0.718/0.848	0.817	0.817
VGG16Inception [42]	0.954	0.910/0.954	0.938	0.938	0.889	0.788/0.888	0.857	0.856
ViT [43]	0.841	0.705/0.840	0.801	0.800	0.832	0.691/0.831	0.803	0.803
Swin-Transformer [44]	0.876	0.766/0.875	0.838	0.837	0.846	0.724/0.851	0.791	0.789
Dinov2_Vitb14 [45]	0.853	0.726/0.852	0.802	0.800	0.885	0.782/0.885	0.840	0.839
RseNet50 [9]	0.960	0.922/0.960	0.947	0.947	0.925	0.856/0.925	0.918	0.918
<b>DALAResNet50</b>	<b>0.979</b>	<b>0.958/0.979</b>	<b>0.98</b>	<b>0.98</b>	<b>0.943</b>	<b>0.891/0.944</b>	<b>0.945</b>	<b>0.945</b>

Note: In the table, the DenseNet-121 model indicates that employed a pre-trained DenseNet-121 model for transfer learning.

**TABLE 7. The count of parameters in the network model and the time it takes to converge.**

Network Models	Convergence Time (seconds)				Total Parameters	Average Time
	40X	100X	200X	400X		
SEResNet50 [39]	2696.22	2814.30	2711.89	2356.18	27073090	2644.65
DenseNet121 [40]	2352.46	2643.79	2423.36	2078.34	<b>9028970</b>	2347.49
VGG16 [41]	3212.95	3182.54	3011.53	2640.19	134268738	3011.80
VGG16Inception [42]	3074.99	3253.50	3303.12	2682.61	38139938	3078.56
ViT [43]	2932.11	3022.54	3013.86	2691.16	51375106	2914.92
Swin-Transformer [44]	3020.11	3132.42	2940.98	2592.96	86745274	2921.62
Dinov2_Vitb14 [45]	2895.02	2303.25	2245.98	2017.15	86582018	2365.35
ResNet50 [9]	2920.53	2933.26	2307.94	2097.33	21797672	2564.77
<b>DALAResNet50</b>	<b>2133.02</b>	<b>2319.50</b>	<b>1990.58</b>	<b>1896.82</b>	25611842	<b>2084.98</b>

Note: In the table, the DenseNet-121 model indicates that a pre-trained DenseNet-121 model was employed for transfer learning.

small sample data.

VGG16 [41]: This model is from Simonyan and Zisserman and was released in 2014. It is known for its clean structure and thoughtful design philosophy and is widely used for image classification and feature extraction tasks, relying mainly on deeply stacked convolutional layers.

VGG16Inception [42]: The model is presented by M. Saini and S. Susan. The article delves into a deep learning model called "VGGIN-Net," which is mainly applied to analyze imbalanced breast cancer datasets. The study introduces a new deep learning framework that incorporates transfer learning to address the problem of category imbalance in biomedical datasets, applied explicitly to the BreakHis breast cancer dataset. The model uses a pre-trained network to migrate learned weights from one domain to another to reduce training time and computational cost.

ViT (Vision Transformer) [43]: Proposed by Dosovitskiy et al. in 2020, it has gained widespread attention by successfully applying the Transformer architecture to image recognition tasks. This model has shown great strength in image recognition.

Swin-Transformer [44]: Liu et al. created this model in 2021,

and its performance in various vision tasks is outstanding. This model is unique in that it solves the computational and memory problems that can be encountered when processing large images.

Dinov2\_Vitb14 [45]: Proposed in 2023 by a team of researchers at Facebook, these models contain a pre-training dataset of 142 million unlabelled images to obtain efficient visual properties demonstrating general solid performance.

Each of the above models has uniqueness and excellent image classification and vision tasks. To emphasize the effectiveness of the proposed approach, an in-depth comparison of all these models has been conducted, achieving significant improvements in various evaluation metrics.

### E. EXPERIMENT METRICS

Used four metrics, Accuracy [46]–[48], F1 Score [49], Imbalance Balanced Accuracy (IBA) [50], and Geometric Mean (GMean) [51], to assess the performance of the model holistically. Below is an introduction to these metrics:

- 1) Accuracy is one of the most intuitive and commonly used metrics for evaluating the overall performance of a model. It calculates the proportion of all samples (whether

positive or negative) that were predicted correctly relative to the total number of samples [46]–[48].

- 2) The F1 Score is a crucial metric that combines precision and recall, providing a comprehensive measure of a model's ability to classify positive and negative instances. This is especially useful for imbalanced datasets where positive and negative samples differ significantly [52].
- 3) IBA is a metric for evaluating the performance of classification models on imbalanced datasets, adjusting standard accuracy to more fairly account for the model's ability to identify both majority and minority classes, ensuring the performance assessment reflects classification effectiveness across all categories. [53].
- 4) GMean is a metric that calculates the geometric mean of individual class accuracies, indicating a model's capability to address category imbalance. It effectively equalizes the performance assessment for both dominant and infrequent categories, emphasizing the model's comprehensive efficiency in handling variances in class distribution. This metric is in scenarios where class imbalance could significantly skew the performance metrics, ensuring that the model's ability to classify less represented classes correctly is adequately considered in its overall [54].

Table 6 showcases the model's performance on the test set at various image resolutions (40X, 100X, 200X, and 400X). Across these resolutions, the model consistently outperforms nine other popular networks regarding accuracy, F1 score, IBA, and GMean. This consistency underlines the network's significant advantage and underscores its potential for medical image classification tasks.

Table 7 compares the model against eight others regarding parameter count and convergence speed. While DenseNet-121 has the fewest parameters, the proposed model achieves the shortest convergence times, exhibiting the fastest average speed across all resolutions (40X, 100X, 200X, and 400X). This further reinforces the proposed model's efficiency and strong potential for medical image classification, highlighting superior performance and effectiveness.

## F. ABLATION STUDY

In this ablation study, we compared the performance of the DALAResNet50 model and the standard ResNet50 model for benign and malignant classification at 40x, 100x, 200x, and 400x magnifications. As shown in Table 6, the DALAResNet50 model outperformed the standard ResNet50 model across all metrics, including accuracy, precision, recall, F1 score, IBA, and GMean. Additionally, we provided confusion matrices for both models on the test set, illustrated in Fig. 6. The results demonstrated that the DALAResNet50 model exhibited higher sensitivity and specificity at all magnifications, significantly reducing the number of false positives and false negatives. These findings suggest that the DALAResNet50 model surpasses the standard ResNet50 model in terms of classification accuracy and reliability.

## V. DT GRAD-CAM

The interpretability of deep learning models is crucial, particularly in areas such as breast cancer diagnosis. Grad-CAM is a popular technique for visualizing class-specific regions of interest in images. This article introduces an enhancement called DT Grad-CAM (Dynamic Threshold Grad-CAM), which improves Grad-CAM by applying adaptive thresholds using the Otsu method, enhancing the visualizations' clarity and relevance.

### A. DT GRAD-CAM METHOD

The DT Grad-CAM method enhances the traditional Grad-CAM approach through several steps. Each step improves the visualization of class-specific regions, making the results more interpretable and relevant for diagnostic purposes.

#### 1. GRAD-CAM CALCULATION

Grad-CAM uses the following formula to compute the gradient-weighted feature map:

$$L_c^{\text{Grad-CAM}} = \text{ReLU} \left( \sum_k \alpha_k^c A^k \right) \quad (5)$$

where:

- $L_c^{\text{Grad-CAM}}$  is the Grad-CAM heatmap for class  $c$ .
- $A^k$  is the  $k$ -th feature map of the convolutional layer.
- $\alpha_k^c$  is the weight for feature map  $A^k$ , defined as the global average pooling of the gradients of class  $c$  with respect to  $A^k$ :

$$\alpha_k^c = \frac{1}{Z} \sum_i \sum_j j \frac{\partial y^c}{\partial A_{ij}^k} \quad (6)$$

where:

- $y^c$  is the score for class  $c$ .
- $\frac{\partial y^c}{\partial A_{ij}^k}$  is the gradient of the score for class  $c$  with respect to the feature map  $A^k$  at location  $(i, j)$ .
- $Z$  is the total number of elements in the feature map (i.e., width times height).

This step leverages the gradient information to highlight the most important features contributing to the class prediction, providing an intuitive visual explanation of the model's decision-making process.

#### 2. OTSU THRESHOLD CALCULATION

After generating the Grad-CAM heatmap, DT Grad-CAM applies Otsu's method to determine the optimal threshold value. Otsu's method calculates the threshold  $T$  that maximizes the between-class variance:

$$\sigma_B^2(T) = \omega_1(T)\omega_2(T)[\mu_1(T) - \mu_2(T)]^2 \quad (7)$$

where:

- $\sigma_B^2(T)$  is the between-class variance for threshold  $T$ .
- $\omega_1(T)$  and  $\omega_2(T)$  are the probabilities of foreground and background pixels at threshold  $T$ , respectively.

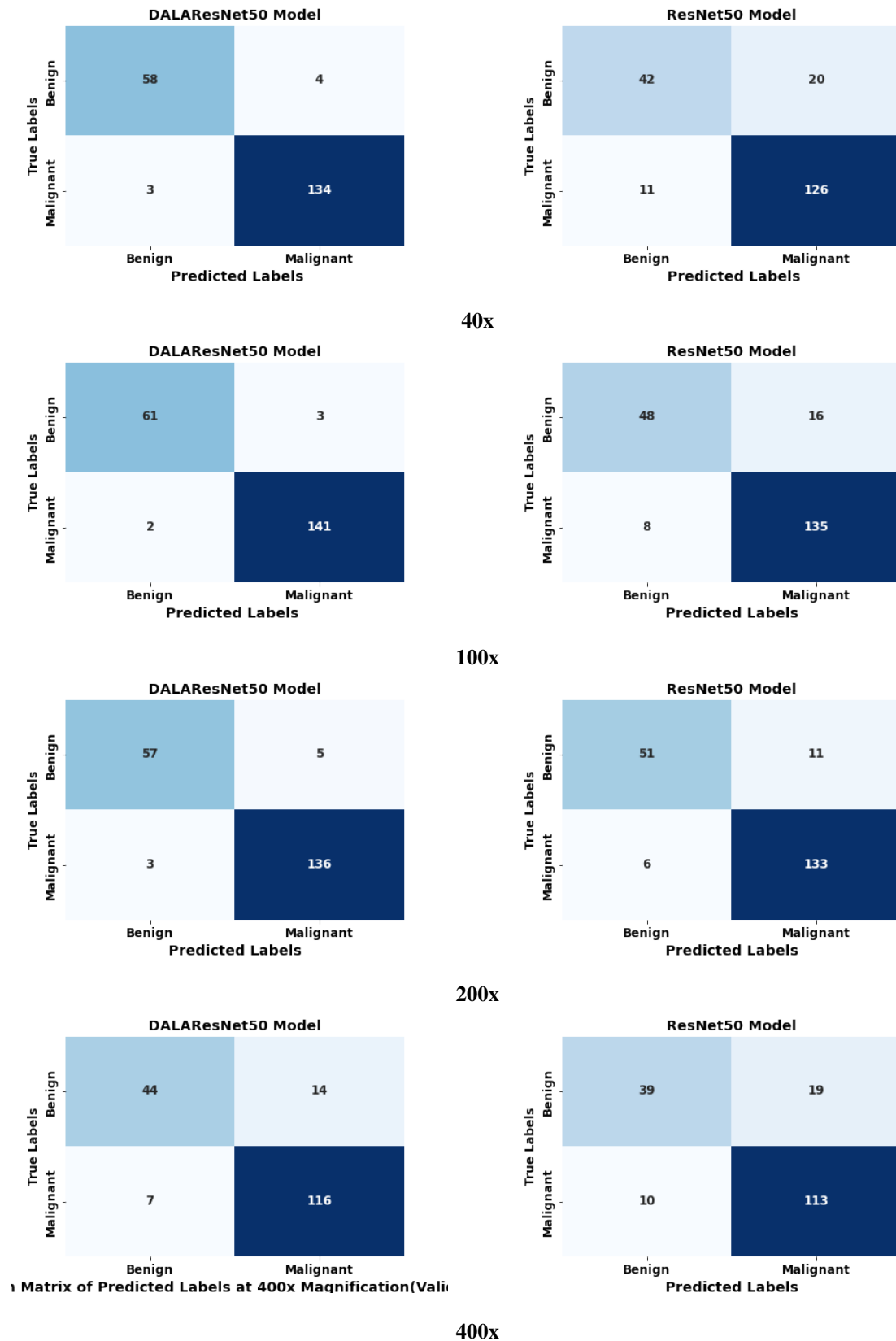
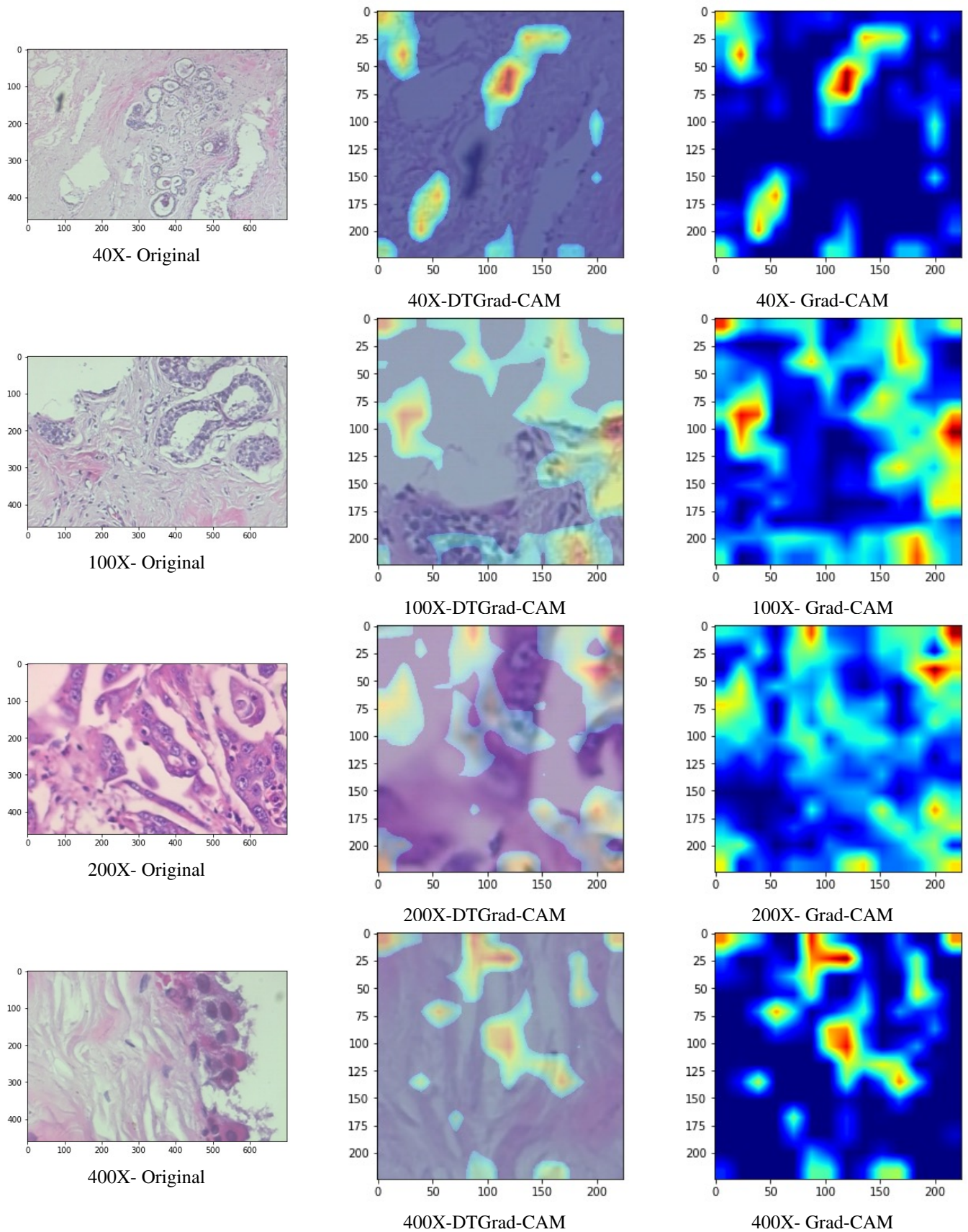


FIGURE 6. Comparison of the confusion matrices of the DALAResNet50 model and the standard ResNet50 model.



**FIGURE 7.** Comparison of Original Histopathology Images with DT Grad-CAM and Grad-CAM Visualizations at Different Magnifications

- $\mu_1(T)$  and  $\mu_2(T)$  are the means of the foreground and background pixels at threshold  $T$ , respectively.

By iterating through all possible thresholds  $T$ , the one that maximizes  $\sigma_B^2(T)$  is selected as the Otsu threshold.

Using Otsu's method allows for adaptive thresholding based on the image's specific characteristics, ensuring that the most relevant regions are highlighted dynamically rather than relying on a fixed threshold.

### 3. THRESHOLDING

The Otsu threshold is then used to binarize the Grad-CAM heatmap:

$$L_c^{\text{Threshold}}(x, y) = \begin{cases} L_c^{\text{Grad-CAM}}(x, y) & \text{if } L_c^{\text{Grad-CAM}}(x, y) > T \\ 0 & \text{otherwise} \end{cases} \quad (8)$$

where:

- $L_c^{\text{Threshold}}$  is the thresholded Grad-CAM heatmap.
- $T$  is the optimal threshold determined by Otsu's method.

This thresholding step ensures that only the most significant regions in the Grad-CAM heatmap are highlighted, improving the visualization's clarity and focus by removing less relevant areas.

### B. COMPARISON BETWEEN DT GRAD-CAM AND GRAD-CAM VISUALIZATION

Fig. 5 illustrates a side-by-side comparison of original images, DT Grad-CAM visualizations, and traditional Grad-CAM visualizations at various magnifications (40X, 100X, 200X, and 400X). Each row shows the original image, the DT Grad-CAM visualization, and the Grad-CAM visualization, respectively. The DT Grad-CAM method consistently provides clearer and more focused representations of significant regions across all magnifications. By applying adaptive thresholding using Otsu's method, DT Grad-CAM reduces noise and enhances the visibility of critical areas, which is particularly evident when comparing the middle columns (DT Grad-CAM) with the right columns (Grad-CAM). This adaptive approach results in sharper and more interpretable visualizations, highlighting the relevant features more distinctly and minimizing the influence of irrelevant regions. Consequently, DT Grad-CAM offers superior clarity and relevance, making it a valuable tool for improving model interpretability, especially in diagnostic applications such as breast cancer imaging.

Table 8 provides a detailed comparison between DT Grad-CAM and Grad-CAM, highlighting the key differences and advantages of DT Grad-CAM. The adaptive thresholding in DT Grad-CAM enhances the clarity and relevance of the visualizations by minimizing noise and focusing on the most significant features. The clarity of visualization is significantly improved in DT Grad-CAM by isolating the key areas of interest and reducing the influence of less relevant regions. This enhancement in clarity directly translates to better interpretability, as DT Grad-CAM offers a sharper and more meaningful highlight of critical regions, making it easier for users

to understand and interpret the model's focus areas. Noise reduction is another major advantage of DT Grad-CAM, as it effectively reduces noise in the visualization, ensuring that only the most pertinent areas are highlighted. This is particularly useful in diagnostic applications, such as breast cancer imaging, where precise and clear visualization of important regions is crucial for accurate analysis. In contrast, traditional Grad-CAM lacks these adaptive enhancements, often resulting in more noise and less precise highlighting of important regions, which can obscure the interpretation and impact the accuracy of diagnostic applications.

## VI. PERFORMANCE EVALUATION AND VISUALIZATION

To effectively monitor the model's performance and gain insights into the training process, it is essential to concentrate on various crucial metrics, such as training loss, validation loss, training accuracy, and validation accuracy. Visualizing these metrics offers a comprehensive view of the model's training behaviour. An in-depth analysis of these key metrics and their implications is outlined below:

### A. LOSS ANALYSIS

This study deployed a DALAResNet50 model for the classification of breast cancer. Critical metrics for assessing model performance and understanding the training dynamics include training loss and validation loss [55]–[57]. These metrics are crucial for evaluating the model's effectiveness, and their graphical representation offers a detailed insight into the training progression.

Fig. 6 illustrates the fluctuations in training and validation losses across varying numbers of training iterations at different image magnifications (40X, 100X, 200X, and 400X). The x-axis represents the number of training iterations, while the y-axis reflects the loss values. Line plots demonstrate the trends in training and validation losses, with error bars on each point indicating the standard deviation of these values.

Training and validation losses consistently decline, indicating the model's successful learning and adaptation to the dataset. This downward trend is encouraging, as it signals ongoing improvement in task performance. In the later training phases, the validation loss stabilizes, suggesting that the model avoids overfitting on the validation dataset and exhibits robust generalization capabilities to unseen data.

### B. ACCURACY ANALYSIS

In Fig. 7, the progression of training and validation accuracy across various image resolutions (40X, 100X, 200X, and 400X) is illustrated [58]. The horizontal axis indicates the number of training iterations, whereas the vertical axis displays accuracy levels. A line graph is utilized to depict the trend in accuracy, with error bars included to illustrate the standard deviation of the accuracy figures.

After meticulous analysis, the following outcomes have been derived: Training and validation accuracy undergo a gradual ascent, showcasing the model's persistent learning and adaptation throughout the training process. This upward trajec-

**TABLE 8. Comparison between DT Grad-CAM and Grad-CAM**

Feature	DT Grad-CAM	Grad-CAM
Adaptive Thresholding	Utilizes Otsu's method to dynamically determine the optimal threshold, enhancing the clarity and relevance of the highlighted regions by minimizing noise and focusing on the most significant features.	Does not employ adaptive thresholding, often leading to more noise and less precise highlighting of important regions.
Clarity of Visualization	Provides clearer and more focused visualizations by isolating the key areas of interest and reducing the influence of less relevant regions.	Visualizations may be more dispersed and less distinct, making it harder to interpret the significant regions accurately.
Interpretability	Enhances model interpretability by offering a sharper and more meaningful highlight of critical regions, making it easier for users to understand and interpret the model's focus areas.	Provides a basic level of interpretability but can be less effective in highlighting the most relevant features clearly.
Noise Reduction	Effectively reduces noise in the visualization, ensuring that only the most pertinent areas are highlighted, thus improving the overall quality of the heatmap.	Higher levels of noise can obscure the interpretation, as less important regions may also be highlighted.
Relevance in Diagnostic Applications	Particularly useful in diagnostic applications, such as breast cancer imaging, where precise and clear visualization of important regions is crucial for accurate analysis.	Useful but may lack the precision required for detailed diagnostic purposes, potentially impacting the accuracy of interpretations.

tory suggests that the model is advancing in comprehending and classifying the data. Additionally, the validation accuracy maintains stability, especially in the later stages of training, implying that the model avoids overfitting to the training data and can generalize effectively to unseen data. These findings are pivotal in comprehending the model's performance and can facilitate further optimization for enhanced breast cancer classification results.

## VII. DALARESNET50'S FUTURE THERAPEUTIC IMPACT AND INTEGRATION INTO EXISTING DIAGNOSTIC PROCESSES

DALAResNet50 model promises to significantly impact the future of breast cancer treatment by enhancing diagnostic accuracy and providing clear, interpretable visualizations through the integration of DT Grad-CAM. As healthcare systems increasingly adopt artificial intelligence (AI) technologies, this model can streamline diagnostic workflows, reduce diagnostic errors, and facilitate earlier detection of breast cancer, which is crucial for improving patient outcomes.

Incorporating DALAResNet50 into existing diagnostic processes can enhance the efficiency and accuracy of histopathology evaluations. Pathologists can leverage the model's high classification accuracy to identify cancerous tissues more confidently, thus supporting more accurate and timely diagnoses. The use of DT Grad-CAM further aids pathologists by providing visual explanations for the model's predictions, highlighting critical regions within histopathology images, and ensuring transparency in the diagnostic process.

Moreover, the DALAResNet50 model can serve as a valuable second-opinion tool, assisting pathologists in confirming their initial diagnoses and potentially identifying cases that may require further review. This integration can lead to a more robust diagnostic process, where AI augments human expertise, reducing the cognitive load on pathologists and minimiz-

ing the risk of oversight.

As the model continues to be refined and validated with larger and more diverse datasets, its application can extend beyond breast cancer to other types of histopathological analyses. This scalability and adaptability make DALAResNet50 a versatile tool in the broader field of medical diagnostics.

In the future, integrating DALAResNet50 with electronic health record (EHR) systems can further streamline patient management by providing seamless access to diagnostic results and AI-generated insights. This integration would facilitate multidisciplinary collaboration among healthcare providers, ensuring that treatment plans are informed by the most accurate and comprehensive diagnostic information available.

Overall, the DALAResNet50 model, combined with DT Grad-CAM's interpretability, holds great promise for transforming breast cancer diagnosis and treatment. Its integration into existing diagnostic workflows can lead to more precise, reliable, and efficient medical care, ultimately enhancing patient outcomes and advancing the field of histopathology.

## VIII. SUMMARY AND CONCLUSIONS

This paper proposed a DALAResNet50 model for classifying medical histopathology tissue images, mainly when dealing with limited-scale imbalanced breast cancer histopathology image datasets. The ResNet50 model incorporates the lightweight attention mechanism to optimize the pre-trained deep network layer. The performance evaluation includes metrics such as accuracy, F1 score, IBA, and GMean, which allow for a comprehensive assessment of this paper's model performance compared to existing techniques. The experimental results highlight significant advantages, particularly when addressing the challenges of imbalanced breast cancer datasets. The model demonstrates improved robustness, generalization, faster convergence during training, and effective prevention of overfitting. These findings provide a solid ba-

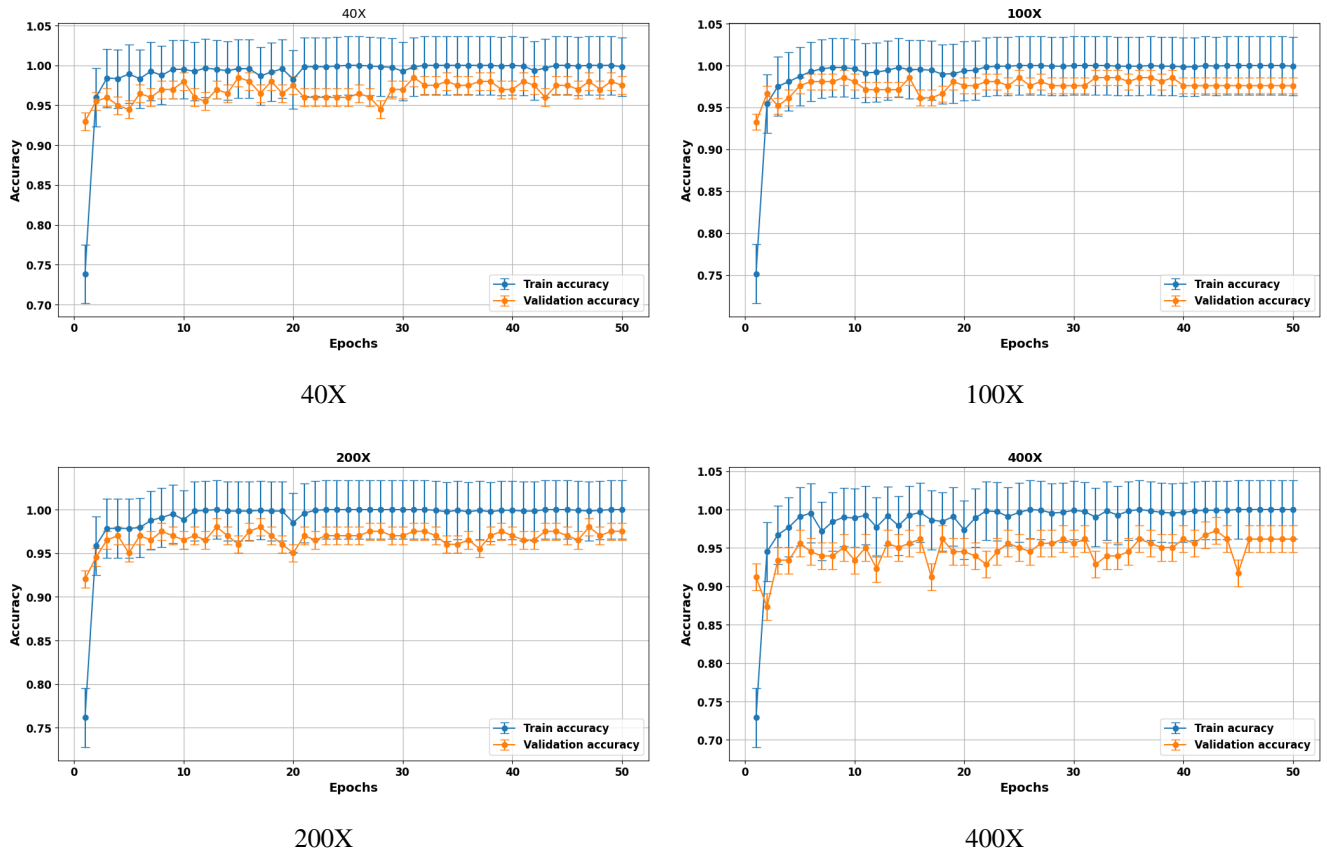


Fig. 8. Training and validation accuracy with error bars

sis for enhancing classification accuracy. Furthermore, this study introduces the DT Grad-CAM method to address the interpretability challenges often associated with deep learning models. DT Grad-CAM enhances the traditional Grad-CAM approach by applying adaptive thresholding using Otsu’s method, which provides clearer and more focused visualizations of significant regions. This method improves the clarity and relevance of the highlighted areas, making it easier for medical experts to interpret the model’s predictions and understand the critical features contributing to the classification. The integration of DT Grad-CAM with DALAResNet50 ensures high classification performance and enhanced interpretability, crucial for reliable and transparent breast cancer diagnosis. In future research, more investigations into breast multiclassification problems are planned.

REFERENCES

[1] S. Kharya, “Using data mining techniques for diagnosis and prognosis of cancer disease,” *arXiv preprint arXiv:1205.1923*, 2012.  
 [2] M. I. Razzak, S. Naz, and A. Zaib, “Deep learning for medical image processing: Overview, challenges and the future,” *Classification in BioApps: Automation of Decision Making*, pp. 323–350, 2018.  
 [3] L. Alzubaidi, J. Zhang, A. J. Humaidi, A. Al-Dujaili, Y. Duan, O. Al-Shamma, J. Santamaría, M. A. Fadhel, M. Al-Amidie, and L. Farhan, “Review of deep learning: Concepts, cnn architectures, challenges, applications, future directions,” *Journal of big Data*, vol. 8, pp. 1–74, 2021.  
 [4] R. A. Dar, M. Rasool, A. Assad et al., “Breast cancer detection using deep learning: Datasets, methods, and challenges ahead,” *Computers in biology*

*and medicine*, p. 106073, 2022.  
 [5] N. S. Ismail and C. Sovuthy, “Breast cancer detection based on deep learning technique,” in *2019 International UNIMAS STEM 12th engineering conference (EnCon)*. IEEE, 2019, pp. 89–92.  
 [6] S. S. Koshy, L. J. Anbarasi, M. Jawahar, and V. Ravi, “Breast cancer image analysis using deep learning techniques—a survey,” *Health and Technology*, vol. 12, no. 6, pp. 1133–1155, 2022.  
 [7] V. O. Adedayo-Ajayi, R. O. Ogundokun, A. E. Tunbosun, M. O. Adebisi, and A. A. Adebisi, “Metastatic breast cancer detection using deep learning algorithms: A systematic review,” in *2023 International Conference on Science, Engineering and Business for Sustainable Development Goals (SEB-SDG)*, vol. 1. IEEE, 2023, pp. 1–5.  
 [8] Y. LeCun, L. Bottou, Y. Bengio, and P. Haffner, “Gradient-based learning applied to document recognition,” *Proceedings of the IEEE*, vol. 86, no. 11, pp. 2278–2324, 1998.  
 [9] K. He, X. Zhang, S. Ren, and J. Sun, “Deep residual learning for image recognition,” in *Proceedings of the IEEE conference on computer vision and pattern recognition*, 2016, pp. 770–778.  
 [10] J. Xu, Z. Li, B. Du, M. Zhang, and J. Liu, “Reluplex made more practical: Leaky relu,” in *2020 IEEE Symposium on Computers and communications (ISCC)*. IEEE, 2020, pp. 1–7.  
 [11] M. Goyal, R. Goyal, and B. Lall, “Learning activation functions: A new paradigm for understanding neural networks,” *arXiv preprint arXiv:1906.09529*, 2019.  
 [12] H. Zhou, Z. Liu, T. Li, Y. Chen, W. Huang, and Z. Zhang, “Classification of precancerous lesions based on fusion of multiple hierarchical features,” *Computer methods and programs in biomedicine*, vol. 229, p. 107301, 2023.  
 [13] S. M. Anwar, M. Majid, A. Qayyum, M. Awais, M. Alnowami, and M. K. Khan, “Medical image analysis using convolutional neural networks: a review,” *Journal of medical systems*, vol. 42, pp. 1–13, 2018.  
 [14] Y. Yu and F. Liu, “Dense connectivity based two-stream deep feature fusion framework for aerial scene classification,” *Remote Sensing*, vol. 10, no. 7, p. 1158, 2018.



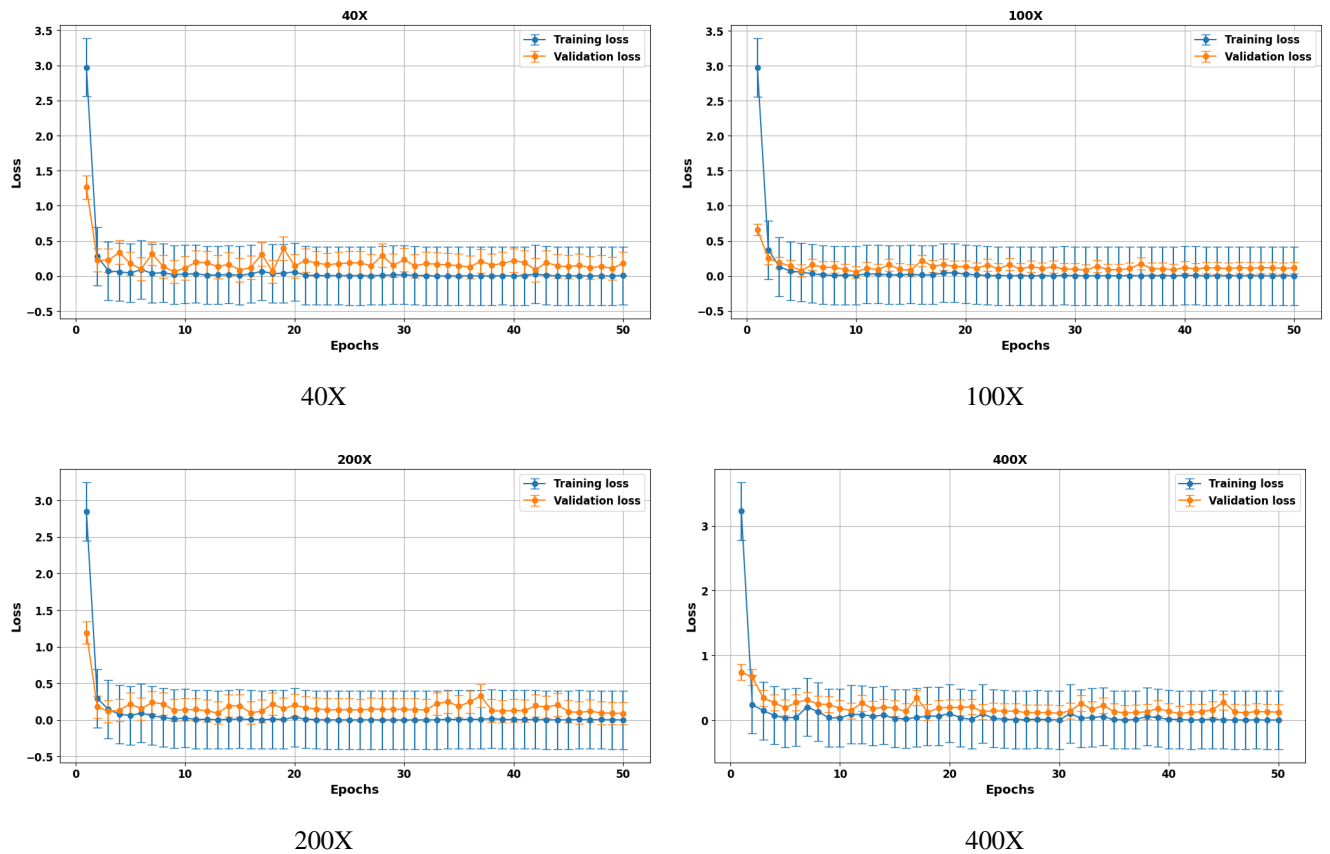
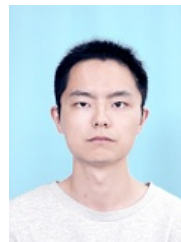


Fig. 9. Training and validation loss with error bars

- [15] Z. Chen, Y. Song, Y. Ma, G. Li, R. Wang, and H. Hu, "Interaction in transformer for change detection in vhr remote sensing images," *IEEE Transactions on Geoscience and Remote Sensing*, 2023.
- [16] A. Krizhevsky, I. Sutskever, and G. E. Hinton, "Imagenet classification with deep convolutional neural networks," *Advances in neural information processing systems*, vol. 25, 2012.
- [17] E. L. Omonigho, M. David, A. Adejo, and S. Aliyu, "Breast cancer: tumor detection in mammogram images using modified alexnet deep convolution neural network," in *2020 international conference in mathematics, computer engineering and computer science (ICMCECS)*. IEEE, 2020, pp. 1–6.
- [18] M. S. Nazir, U. G. Khan, A. Mohiyuddin, M. S. Al Reshan, A. Shaikh, M. Rizwan, and M. Davidekova, "A novel cnn-inception-v4-based hybrid approach for classification of breast cancer in mammogram images," *Wireless Communications and Mobile Computing*, vol. 2022, pp. 1–10, 2022.
- [19] I. Nedjar, M. Brahim, S. Mahmoudi, K. A. Ayad, and M. A. Chikh, "Exploring regions of interest: Visualizing histological image classification for breast cancer using deep learning," *arXiv preprint arXiv:2305.20058*, 2023.
- [20] G. Huang, Z. Liu, L. Van Der Maaten, and K. Q. Weinberger, "Densely connected convolutional networks," in *Proceedings of the IEEE conference on computer vision and pattern recognition*, 2017, pp. 4700–4708.
- [21] Y. Jiménez Gaona, M. J. Rodríguez-Alvarez, H. Espino-Morato, D. Castillo Malla, and V. Lakshminarayanan, "Densenet for breast tumor classification in mammographic images," in *International Conference on Bioengineering and Biomedical Signal and Image Processing*. Springer, 2021, pp. 166–176.
- [22] H. A. Khikani, N. Elazab, A. Elgarayhi, M. Elmogy, and M. Sallah, "Breast cancer classification based on histopathological images using a deep learning capsule network," *arXiv preprint arXiv:2208.00594*, 2022.
- [23] M. Alruwaili and W. Gouda, "Automated breast cancer detection models based on transfer learning," *Sensors*, vol. 22, no. 3, p. 876, 2022.
- [24] S. Arooj, M. Zubair, M. F. Khan, K. Alissa, M. A. Khan, A. Mosavi et al., "Breast cancer detection and classification empowered with transfer learning," *Frontiers in Public Health*, vol. 10, p. 924432, 2022.
- [25] V. Azevedo, C. Silva, and I. Dutra, "Quantum transfer learning for breast cancer detection," *Quantum Machine Intelligence*, vol. 4, no. 1, p. 5, 2022.
- [26] Y. Chen, C. Liu, W. Huang, S. Cheng, R. Arcucci, and Z. Xiong, "Generative text-guided 3d vision-language pretraining for unified medical image segmentation," *arXiv preprint arXiv:2306.04811*, 2023.
- [27] C. Liu, S. Cheng, C. Chen, M. Qiao, W. Zhang, A. Shah, W. Bai, and R. Arcucci, "M-flag: Medical vision-language pre-training with frozen language models and latent space geometry optimization," in *International Conference on Medical Image Computing and Computer-Assisted Intervention*. Springer, 2023, pp. 637–647.
- [28] Z. Wan, C. Liu, M. Zhang, J. Fu, B. Wang, S. Cheng, L. Ma, C. Quilodrán-Casas, and R. Arcucci, "Med-unic: Unifying cross-lingual medical vision-language pre-training by diminishing bias," *arXiv preprint arXiv:2305.19894*, 2023.
- [29] C. Liu, S. Cheng, M. Shi, A. Shah, W. Bai, and R. Arcucci, "Imitate: Clinical prior guided hierarchical vision-language pre-training," *arXiv preprint arXiv:2310.07355*, 2023.
- [30] N. S. Ismail and C. Sovuthy, "Breast cancer detection based on deep learning technique," in *2019 International ANIMAS STEM 12th engineering conference (EnCon)*. IEEE, 2019, pp. 89–92.
- [31] M. I. Mahmud, M. Mamun, and A. Abdelgawad, "A deep analysis of transfer learning based breast cancer detection using histopathology images," in *2023 10th International Conference on Signal Processing and Integrated Networks (SPIN)*. IEEE, 2023, pp. 198–204.
- [32] G. Brauwuers and F. Frasincaer, "A general survey on attention mechanisms in deep learning," *IEEE Transactions on Knowledge and Data Engineering*, 2021.
- [33] J. Kang, L. Liu, F. Zhang, C. Shen, N. Wang, and L. Shao, "Semantic segmentation model of cotton roots in-situ image based on attention mechanism," *Computers and Electronics in Agriculture*, vol. 189, p. 106370, 2021.
- [34] C. C. Ukwuoma, G. C. Urama, Z. Qin, M. B. B. Heyat, H. M. Khan,

- F. Akhtar, M. S. Masadeh, C. S. Ibegbulam, F. L. Delali, and O. AlShorman, "Boosting breast cancer classification from microscopic images using attention mechanism," in *2022 International Conference on Decision Aid Sciences and Applications (DASA)*. IEEE, 2022, pp. 258–264.
- [35] J. Vardhan and G. S. Krishna, "Breast cancer segmentation using attention-based convolutional network and explainable ai," *arXiv preprint arXiv:2305.14389*, 2023.
- [36] B. Xu, J. Liu, X. Hou, B. Liu, J. Garibaldi, I. O. Ellis, A. Green, L. Shen, and G. Qiu, "Look, investigate, and classify a deep hybrid attention method for breast cancer classification," in *2019 IEEE 16th international symposium on biomedical imaging (ISBI 2019)*. IEEE, 2019, pp. 914–918.
- [37] C. Wang, F. Xiao, W. Zhang, S. Huang, W. Zhang, and P. Zou, "Transfer learning and attention mechanism for breast cancer classification," in *2021 17th International Conference on Computational Intelligence and Security (CIS)*. IEEE, 2021, pp. 75–79.
- [38] F. A. Spanhol, L. S. Oliveira, C. Petitjean, and L. Heutte, "A dataset for breast cancer histopathological image classification," *Ieee transactions on biomedical engineering*, vol. 63, no. 7, pp. 1455–1462, 2015.
- [39] J. Hu, L. Shen, and G. Sun, "Squeeze-and-excitation networks," in *Proceedings of the IEEE conference on computer vision and pattern recognition*, 2018, pp. 7132–7141.
- [40] G. Huang, Z. Liu, L. Van Der Maaten, and K. Q. Weinberger, "Densely connected convolutional networks," in *Proceedings of the IEEE conference on computer vision and pattern recognition*, 2017, pp. 4700–4708.
- [41] K. Simonyan and A. Zisserman, "Very deep convolutional networks for large-scale image recognition," *arXiv preprint arXiv:1409.1556*, 2014.
- [42] M. Saini and S. Susan, "Vggin-net: Deep transfer network for imbalanced breast cancer dataset," *IEEE/ACM Transactions on Computational Biology and Bioinformatics*, vol. 20, no. 1, pp. 752–762, 2022.
- [43] A. Dosovitskiy, L. Beyer, A. Kolesnikov, D. Weissenborn, X. Zhai, T. Unterthiner, M. Dehghani, M. Minderer, G. Heigold, S. Gelly et al., "An image is worth 16x16 words: Transformers for image recognition at scale," *arXiv preprint arXiv:2010.11929*, 2020.
- [44] Z. Liu, Y. Lin, Y. Cao, H. Hu, Y. Wei, Z. Zhang, S. Lin, and B. Guo, "Swin transformer: Hierarchical vision transformer using shifted windows," in *Proceedings of the IEEE/CVF international conference on computer vision*, 2021, pp. 10 012–10 022.
- [45] Facebook Research Team, "Dinov2: High-performance visual feature generation model," [Online]. Available: <https://github.com/facebookresearch/dinov2>, 2023.
- [46] C. Zhang, P. Soda, J. Bi, G. Fan, G. Almpandis, S. García, and W. Ding, "An empirical study on the joint impact of feature selection and data resampling on imbalance classification," *Applied Intelligence*, vol. 53, no. 5, pp. 5449–5461, 2023.
- [47] B. Alsinglawi, O. Alshari, M. Alorjani, O. Mubin, F. Alnajjar, M. Novoa, and O. Darwish, "An explainable machine learning framework for lung cancer hospital length of stay prediction," *Scientific reports*, vol. 12, no. 1, p. 607, 2022.
- [48] S. Khan, M. Hayat, S. W. Zamir, J. Shen, and L. Shao, "Striking the right balance with uncertainty," in *Proceedings of the IEEE/CVF Conference on Computer Vision and Pattern Recognition*, 2019, pp. 103–112.
- [49] D. Chicco and G. Jurman, "The advantages of the matthews correlation coefficient (mcc) over f1 score and accuracy in binary classification evaluation," *BMC genomics*, vol. 21, no. 1, pp. 1–13, 2020.
- [50] U. R. Gogoi, G. Majumdar, M. K. Bhowmik, and A. K. Ghosh, "Evaluating the efficiency of infrared breast thermography for early breast cancer risk prediction in asymptomatic population," *Infrared Physics & Technology*, vol. 99, pp. 201–211, 2019.
- [51] I. M. De Diego, A. R. Redondo, R. R. Fernández, J. Navarro, and J. M. Moguerza, "General performance score for classification problems," *Applied Intelligence*, vol. 52, no. 10, pp. 12 049–12 063, 2022.
- [52] F. Maleki, K. Ovens, R. Gupta, C. Reinhold, A. Spatz, and R. Forghani, "Generalizability of machine learning models: Quantitative evaluation of three methodological pitfalls," *Radiology: Artificial Intelligence*, vol. 5, no. 1, p. e220028, 2022.
- [53] M. Saini and S. Susan, "Tackling class imbalance in computer vision: a contemporary review," *Artificial Intelligence Review*, pp. 1–57, 2023.
- [54] M. Hossin and M. N. Sulaiman, "A review on evaluation metrics for data classification evaluations," *International journal of data mining & knowledge management process*, vol. 5, no. 2, p. 1, 2015.
- [55] M. A. Bhuiyan, T. Crovella, A. Paiano, and H. Alves, "A review of research on tourism industry, economic crisis and mitigation process of the loss: Analysis on pre, during and post pandemic situation," *Sustainability*, vol. 13, no. 18, p. 10314, 2021.
- [56] X. Wei, Y. Chen, and Z. Zhang, "Comparative experiment of convolutional neural network (cnn) models based on pneumonia x-ray images detection," in *2020 2nd International Conference on Machine Learning, Big Data and Business Intelligence (MLBDBI)*. IEEE, 2020, pp. 449–454.
- [57] A. S. Ravindran, M. Cestari, C. Malaya, I. John, G. E. Francisco, C. Layne, and J. L. C. Vidal, "Interpretable deep learning models for single trial prediction of balance loss," in *2020 IEEE international conference on systems, man, and cybernetics (SMC)*. IEEE, 2020, pp. 268–273.
- [58] R. Aggarwal, V. Sounderajah, G. Martin, D. S. Ting, A. Karthikesalingam, D. King, H. Ashrafiyan, and A. Darzi, "Diagnostic accuracy of deep learning in medical imaging: a systematic review and meta-analysis," *NPJ digital medicine*, vol. 4, no. 1, p. 65, 2021.
- [59] S. Soomro, A. Niaz, and K. N. Choi, "Grad++ ScoreCAM: Enhancing Visual Explanations of Deep Convolutional Networks using Incremented Gradient and Score-Weighted Methods," *IEEE Access*, 2024.
- [60] Q. Zhang, L. Rao, and Y. Yang, "A novel visual interpretability for deep neural networks by optimizing activation maps with perturbation," in *Proceedings of the AAAI Conference on Artificial Intelligence*, vol. 35, no. 4, pp. 3377–3384, 2021.
- [61] N. H. F. Beebe, "A Complete Bibliography of Publications in ACM Computing Surveys," 2024.



**SUXING LIU** received a Bachelor of Engineering from Anhui Agricultural University and a Master's degree from Xi'an University of Technology, both in China. He is currently a Ph.D. student at the Universiti Sains Malaysia. His primary research area is in medical image processing. He has published several papers in the field of artificial intelligence.

...